VSP – a Quantum Simulator for Engineering Applications

Z. Stanojević, O. Baumgartner, K. Schnass*, M. Karner*, and H. Kosina
Institute for Microelectronics, TU Wien, Gußhausstraße 27–29/E360, 1040 Wien, Austria
*Global TCAD Solutions GmbH, Landhausgasse 4/1a, 1010 Wien, Austria
e-mail: (stanojevic,baumgartner,kosina)@iue.tuwien.ac.at, (k.schnass,m.karner)@globaltcad.com

State of the Art and Motivation

Several software packages exist that are concerned with some aspects of quantum-electronic computation. Codes began to appear in the late nineties as one-dimensional Schrödinger-Poisson solvers. Since then we have seen the development of academic codes such as nextnano^3 [1], NEMO 5 [2], tiberCAD [3], and tdkp/AQUA [4]. These feature accurate modeling of materials through advanced band structure models, and are able to include effects of strain or magnetic fields in the calculation.

Some of these tools are in fact a collection of specialized models tailored to specific tasks and offer little flexibility. Others demand considerable experience in semiconductor physics from the user to operate them properly.

In our work we are seeking to bridge this gap and provide a flexible, highly efficient simulation enviroment for quantum-electronic problems – the Vienna Schrödinger-Poisson framework (VSP) [5]. The framework is aimed at engineers, students with basic knowledge, and the experienced user.

Methods

A number of methods have been developed and adopted for the VSP. At the core of VSP lies a loop that solves the Poisson equation together with a carrier model self-consistently. Different carrier models can be picked: a classical equilibrium distribution, a system of quantized carriers using the parabolic band approximation, or a $\mathbf{k}\cdot\mathbf{p}$ band structure model with an arbitrary number of bands. A unified interface has been developed that allows the user to specifiy any kind of $\mathbf{k}\cdot\mathbf{p}$ Hamiltonian up to second order in $\mathbf{k}$. Arbitrary crystal orientations are possible. Strain and magnetic fields can be included.

Discretization of both real space and $\mathbf{k}$-space is based on a finite volume scheme described in [6], that accurately treats anisotropy, which is important when discretizing $\mathbf{k}\cdot\mathbf{p}$ Hamiltonians. The discretization is independent of the problem dimensionality and each model code works for one, two, and three dimensions. This ensures consistency when comparing problems of different dimensionality. As default, VSP automatically picks the most suitable numerical methods for the problem at hand.

On the numerical side, VSP employs established libraries for solving linear, nonlinear and eigenvalue problems. These are combined with methods that enhance the numerical preformance especially for eigenvalue problems, such as the shift-invert technique or subspace deflation. Scalable parallelization is provided, making the VSP a highly efficient tool.

Results

Figures 1 through 5 show three different devices analyzed using VSP: a p-type MOS capacitor, a p-type FinFET and a STM tip on an lightly p-doped Si substrate covered by a SiO_2 layer. The simulator was set up to obtain the carrier concentration self-consistently with the Poisson equation. The same simulation setup was used for all three devices – only the geometry changed. Three different carrier models were used: (I) classical unconfined carriers, (II) quantum-confined carriers in the parabolic band approximation, and (III) confined carriers with a $\mathbf{k}\cdot\mathbf{p}$ band structure for electrons modeled according to [7] and for holes according to [8] and [9].

Acknowledgment

This work has been supported by the Austrian Science fund through contracts F2509 and I841-N16.

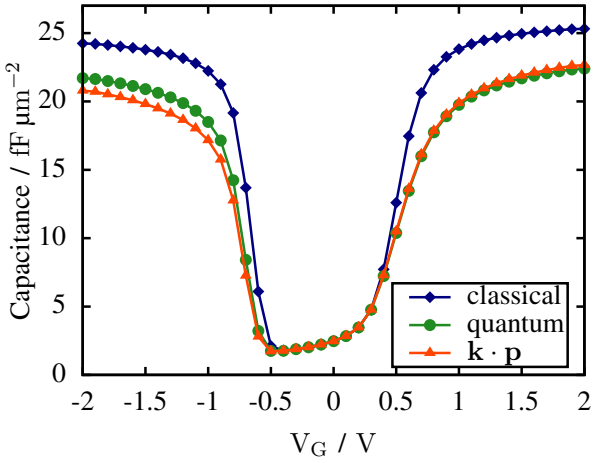

Fig. 1. CV-curve of a p-type MOS capacitor; classical, parabolic band quantum, and $\mathbf{k}\cdot\mathbf{p}$ quantum models are compared; a difference between the effective mass and $\mathbf{k}\cdot\mathbf{p}$ is visible in inversion due to the higher non-parabolicity of the valence band.

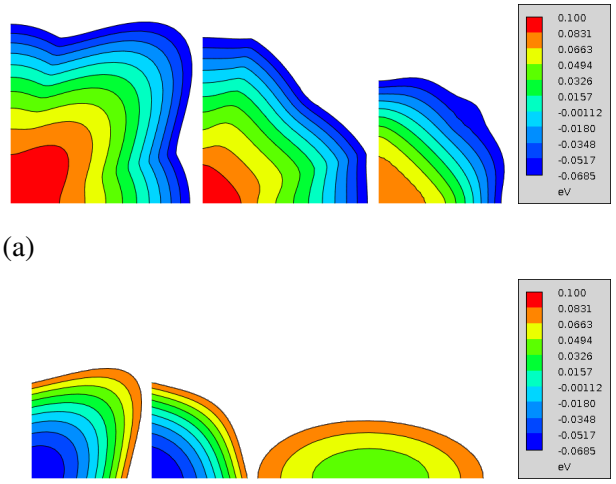

(a)

(b)

Fig. 2. Contour plots of the lowest three subbands in the p-type MOS capacitor calculated using a $\mathbf{k}\cdot\mathbf{p}$ band structure at inversion $V_G = -2\,\mathrm{V}$ (a) and accumulation $V_G = 2\,\mathrm{V}$ (b)

References

[1] S. Birner *et al.*, IEEE T. Electron. Dev. **54**, 2137 (2007).
[2] S. Steiger, *NEMO 5 User Manual*, NCN Purdue Univ.
[3] M. Auf der Maur *et al.*, IEEE T. Electron. Dev. **58**, 1425 (2011).
[4] R. G. Veprek, Ph.D. thesis, ETH Zürich, 2009.
[5] M. Karner *et al.*, J. Comput. Electron. **6**, 179 (2007).
[6] Z. Stanojevic *et al.*, *SISPAD* (2011), pp. 143 –146.
[7] J. C. Hensel *et al.*, Phys. Rev. **138**, A225 (1965).
[8] T. Manku *et al.*, J. Appl. Phys. **73**, 1205 (1993).
[9] Frank L. Madarasz *et al.*, J. Appl. Phys. **52**, 4646 (1981).

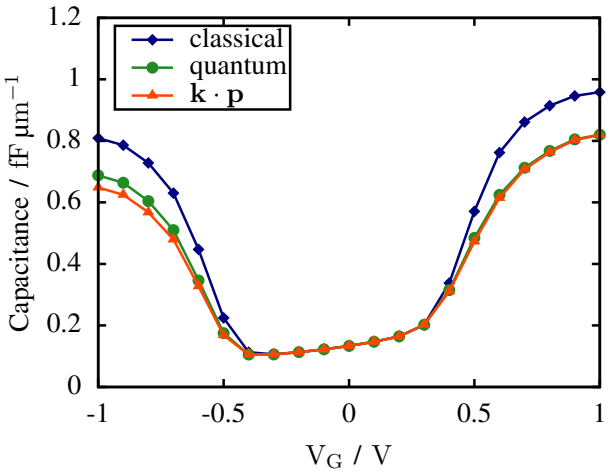

Fig. 3. CV-curve of a p-type FinFET; classical, effective mass quantum, and $\mathbf{k}\cdot\mathbf{p}$ quantum models are compared; here too, the quantum and $\mathbf{k}\cdot\mathbf{p}$ curves differ at inversion.

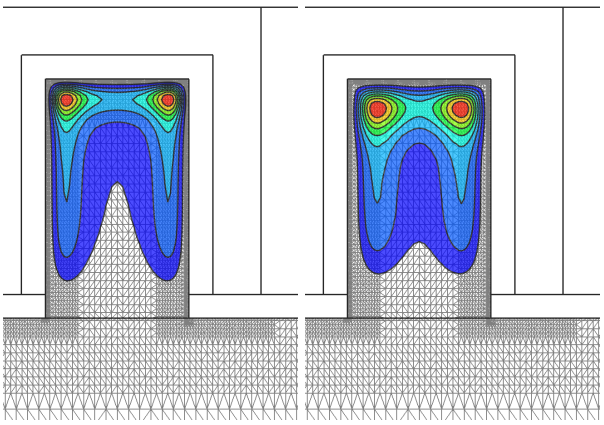

Fig. 4. Hole distribution in the FinFET at inversion $V_G = -1\,\mathrm{V}$; left: parabolic band approximation, right: $\mathbf{k}\cdot\mathbf{p}$ band structure

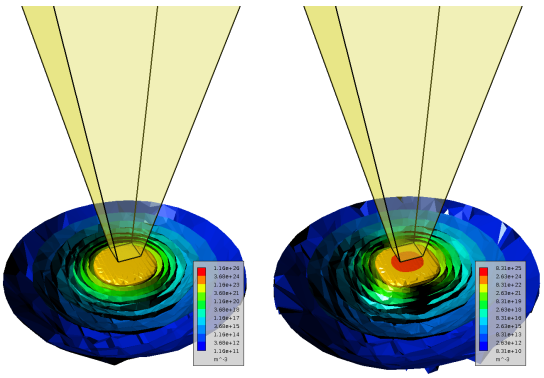

Fig. 5. Electron concentration under a STM tip biased at $4\,\mathrm{V}$; left: parabolic band approximation, right: $\mathbf{k}\cdot\mathbf{p}$ band structure